arXiv:1412.4611v2 [quant-ph] 16 Dec 2014

Supplemental Material for:

Transformation of a single photon field into bunches of pulses

R. N. Shakhmuratov,[1,2] F.G. Vagizov,[1,2,3] V.A. Antonov,[2,4,5] Y.V. Radeonychev,[4,5] and O. Kocharovskaya[3]

[1]*Kazan Physical-Technical Institute, Russian Academy of Sciences, 10/7 Sibirsky Trakt, Kazan 420029 Russia*

[2]*Kazan Federal University, 18 Kremlyovskaya Street, Kazan 420008 Russia*

[3]*Department of Physics and Institute for Quantum Studies, TAMU, College Station, Texas 77843-4242, USA*

[4]*Institute of Applied Physics of the Russian Academy of Sciences, Nizhny Novgorod 603950, Russia*

[5]*N.I. Lobachevsky State University of Nizhny Novgorod, Nizhny Novgorod, 603950, Russia*

(Dated: December 17, 2014)

Abstract

We show here that taking into account the contribution of the nearest satellites of the resonant component removes misfit of our analytical approximation with the exact result for the probability amplitude of the photon, transmitted through the vibrating absorber. We analyze time evolution of the phase difference of the scattered field and the comb. We discuss the scheme how single and two-pulse bunches can be used to simulate spin 1/2 qubit and ququad.

PACS numbers: 42.50.Gy

I. CONTRIBUTION OF NONRESONANT COMPONENTS

If the modulation frequency Ω is much larger than the halfwidth of the absorption line γ_a and only one spectral component of the frequency comb is tuned in resonance with the absorber then one can neglect the interaction with other nonresonant components. Such an idealization works quite well if the spectrum of a single-line radiation source has rapidly falling tails as it is inherent, for example, to the Gaussian spectrum. In case of heralded single photons the spectrum of the radiation field is $a(\omega) = i/(\omega - \omega_s + i\gamma_s)$, see, for example Ref. [1]. This spectrum has long tails falling as $\sim 1/(\omega - \omega_s)$. They appear because the front of the photon wave packet has sharply rising leading edge. Therefore many satellites start wringing immediately after this front comes, however with small amplitudes. As a result the approximate Eq. (5) describes the modulation of a single photon field with small misfit compared with exact Eq. (6) in the main text of the paper. Below we improve fitting by taking into account the interaction with the nearest satellites of the resonant component.

A. Nonaveraged probability amplitude

The propagation of a single line radiation field with carrier frequency ω_s through a single line absorber with resonant frequency ω_a is described by Eq. (6) of the main part of the paper. It is derived by the convolution of the incident field amplitude with the response function (Green function) of a single line absorber, which is

$$R(t) = \delta(t) - \Theta(t) e^{-(i\omega_a + \gamma_a)t} b j_1(bt), \tag{1}$$

where $\delta(t)$ is the Dirac delta function (see, for example, Refs. [1, 2]). According to Eq. (6) of the main part of the manuscript the coherently scattered field amplitude is

$$a_{sct}(t - t_0, l) = -\Theta(t - t_0) b \int_0^{t - t_0} a_A(t - t_0 - \tau, l) j_1(b\tau) e^{-\gamma_a \tau - i\omega_a \tau} d\tau. \tag{2}$$

If the m-component of the frequency comb, Eq. (1) of the main part of the manuscript, is in resonance with the absorber, i.e., $\omega_s = \omega_a + m\Omega$ and $\gamma_s = \gamma_a$, then the amplitude of the coherently scattered field for this component is reduced to

$$a_m(t - t_0, l) = a_L(t - t_0, l) S_m(t - t_0) e^{im(\Omega t + \varphi)}, \tag{3}$$

where for simplification of the notations we drop index *sct*. The contribution of the satellites $\omega_s - (m \pm n)\Omega$, where $n = 1, 2, 3, ...$, was not taken into account in Eq. (5) of the the main part of the manuscript. According to Eq. (2) the amplitudes of the fields, scattered by the satellites are

$$a_{m\pm n}(t - t_0, l) = -a_L(t - t_0, l) J_{m\pm n}(p) e^{i(m\pm n)(\Omega t+\varphi)} b \int_0^{t-t_0} j_1(b\tau) e^{-(\gamma_a-\gamma_s)\tau \mp in\Omega\tau} d\tau. \qquad (4)$$

Then, the exact result, Eq. (6) of the the main part of the manuscript, can be expressed as follows

$$a_{ext}(t, l) = a_A(t, l) + \sum_{n=-\infty}^{+\infty} a_{m+n}(t, l), \qquad (5)$$

where $t_0 = 0$. Comparison of the exact result with the approximation, when only two nearest sattelites ($n = \pm 1$) of the resonant component ($n = 0$) are taken into account, is shown in Fig. 1. In this case misfit is almost negligible. To estimate the contribution of the satellites we calculated the integral

$$K_{\pm n}(t) = b \int_0^t j_1(b\tau) e^{\pm in\Omega\tau - (\gamma_a-\gamma_s)\tau} d\tau \qquad (6)$$

in Eq. (4) with the help of the method, presented in Refs. [3–6]. The result is

$$K_{\pm n}(t) = 1 - e^{-ib/[\pm n\Omega + i(\gamma_a-\gamma_s)]} + M_{\pm n}(t), \qquad (7)$$

$$M_{\pm n}(t) = e^{\pm in\Omega t - (\gamma_a-\gamma_s)t} \sum_{k=1}^{\infty} \left[\frac{-ib}{\pm n\Omega + i(\gamma_a - \gamma_s)}\right]^k j_k(bt), \qquad (8)$$

where $j_k(bt) = J_k\left(2\sqrt{bt}\right)/(bt)^{k/2}$ and $J_k(x)$ is the Bessel function of the k-th order. If $n\Omega \gg b$, then the smallness of the satellites contribution is of the order of $b/n\Omega$. For example, when $b/\Omega = 0.146$, $n = 1$, and $\gamma_a \approx \gamma_b$, then it is already fine approximation if one takes into account only the first term in the sum $M_{\pm 1}(t)$ in Eq. (8), which is proportional to b/Ω, see Fig. 2.

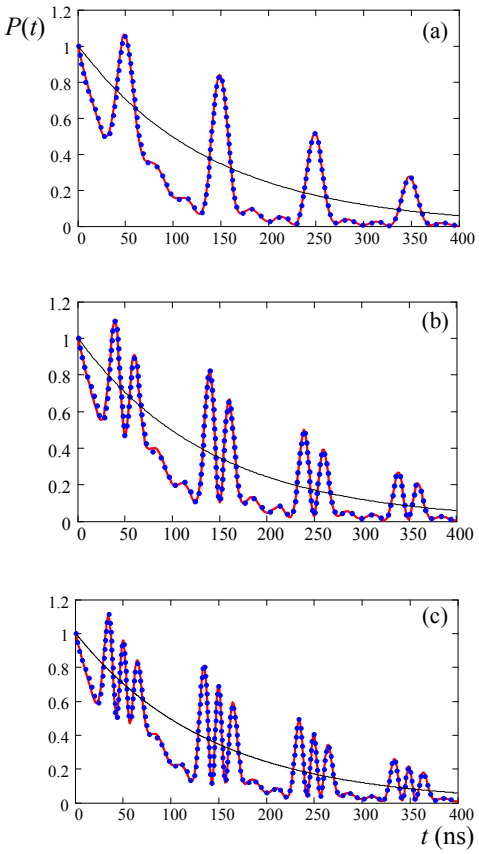

FIG. 1: (color on line) Comparison of the exact result for the probability $P(t)$, derived from Eq. (6) in the main part of the manuscript (solid line in red), with that, which is obtained from Eq. (5), where only the resonant component, $n = 0$, and two nearest satellites, $n = \pm 1$, are taken into account (dotted line in blue). The parameters and notations are the same as in Fig.1 (a-c) of the main part of the manuscript.

B. Averaged probability amplitude

The averaged probability amplitude $\langle P(t - t_0)\rangle_{t_0} = \langle N(t)\rangle$, Eq. (7) in the main part of the paper, is described by the equation (see Refs. [2, 6])

$$\langle N(t)\rangle = \mathrm{Re}\left[1 - 2f_s bF_+(t)\int_{-\infty}^{t} dt' j_1[b(t-t')]/F_+(t') + 2f_s b^2 e^{-2\gamma_a t}\int_{-\infty}^{t} dt' F_-(t') j_1[b(t-t')]\int_{-\infty}^{t'} dt'' j_1[b(t-t'')]/F_+(t'')\right]. \quad (9)$$

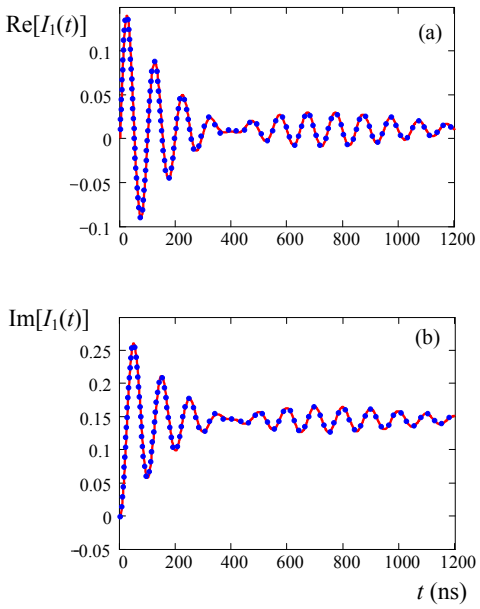

FIG. 2: (color on line) Comparison of the time dependencies of the real (a) and imaginary (b) parts of the integral $K_1(t)$, Eq. (6), (solid line in red) with the equation (7), where only the first term in the sum, Eq. (8), is taken into account (dotted line in blue). The parameters are $b = 1.47$ MHz and $\Omega = 10$ MHz.

where f_s is the recoilless fraction of the source photons and

$$F_{\pm}(t) = \exp\left[-(\gamma_s \pm \gamma_a)t - i(\omega_a - \omega_s)t - ip\sin(\Omega t)\right]. \tag{10}$$

If $\gamma_s = \gamma_a = \gamma$, then Eq. (9) can be simplified as follows

$$\langle N(t)\rangle = 1 - 2f_s b\int_0^{\infty} dt' j_1(bt')e^{-2\gamma t'}\cos\left[\phi(t) - \phi(t-t') - \Delta\omega t'\right]$$
$$+ 2f_s b^2\int_0^{\infty} dt'\int_0^{t'} dt'' j_1(bt')j_1(bt'')e^{-2\gamma t'}\cos\left[\phi(t-t') - \phi(t-t'') + \Delta\omega(t'-t'')\right]. \tag{11}$$

where $\Delta\omega = \omega_s - \omega_a$ is the resonant detuning and $\phi(t) = p\sin(\Omega t + \varphi)$ is the phase modulation of the radiation field in the reference frame of the vibrating absorber.

Equations (9) and (11) are hard to analyze analytically. On the contrary, analytical approximation, given in Eq. (8) of the main part of the paper, helps to estimate the periodicity of pulses, the values of their maxima $\langle N_m\rangle_{\max}$, and the intensity level of the dark windows, $\langle N_m\rangle_{\min}$, where index m indicates that m-th component is in resonance. According to the analytical approximation these values are

$$\langle N_m\rangle_{\max} = [1 + V_m(p)]^2 + J_m^2(p)(\langle N\rangle_{res} - e^{-T_a/2}), \tag{12}$$

$$\langle N_m \rangle_{\min} = [1 - V_m(p)]^2 + J_m^2(p)(\langle N \rangle_{res} - e^{-T_a/2}), \tag{13}$$

where $\langle N \rangle_{res} = \exp(-T_a/2) I_0(T_a/2)$ is proportional to the number of counts per unit time at the output of the single-line absorber if it is tuned in resonance with the source. Comparison of the analytical approximation, Eq. (8) in the main part of the paper, with the exact expression, Eq. (11), for the number of counts at the output of the vibrating absorber, is shown in Fig. 3, along with the values $\langle N_m \rangle_{\max}$, $\langle N_m \rangle_{\min}$, and $\langle N \rangle_{res}$, which are $\langle N_1 \rangle_{\max} = 2.089$, $\langle N_1 \rangle_{\min} = 0.397$ for $\Delta = \Omega$ and $p = 1.8$; $\langle N_2 \rangle_{\max} = 1.877$, $\langle N_2 \rangle_{\min} = 0.463$ for $\Delta = 2\Omega$ and $p = 3.1$; $\langle N_3 \rangle_{\max} = 1.768$, $\langle N_3 \rangle_{\min} = 0.504$ for $\Delta = 3\Omega$ and $p = 4.2$. These values are obtained if modulation frequency is $\Omega = 10$ MHz and $T_a = 5.2$, when $\langle N \rangle_{res} = 0.264$. The maximum intensity of the pulses exceeds almost two times the radiation intensity without absorber. Minimum intensity in the dark windows $\langle N_m \rangle_{\min}$ is almost an order of magnitude smaller than the maximum pulse intensity $\langle N_m \rangle_{\max}$ and slightly exceeds the intensity level of the radiation field, transmitted through the resonant absorber not vibrating, $\langle N \rangle_{res}$. However their difference $\langle N_m \rangle_{min} - \langle N \rangle_{res}$ rises with increase of the value of the modulation index from $p = 1.8$ to $p = 4.2$.

It is possible to improve the analytical approximation, given in Eq. (8) of the main part of the paper, if the contribution of two nearest satellites of the resonant component are taken into account, i.e.,

$$a_{apx}(t,l) = a_A(t,l) + a_m(t,l) + a_{m+1}(t,l) + a_{m-1}(t,l). \tag{14}$$

In the corresponding probability amplitude $P_{apx}(t) = |a_{apx}(t,l)|^2$ we can make further simplification neglecting the terms $|a_{m+1}(t,l) + a_{m-1}(t,l)|^2$ and $2\,\mathrm{Re}\left\{ [a_{m+1}(t,l) + a_{m-1}(t,l)]\, a_L(t,l) J_m\left(2\sqrt{bt}\right) e^{im(\Omega t+\varphi)} \right\}$ since their contribution into the averaged probability $\langle P_{apx}(t-t_0) \rangle_{t_0}$ is small. The contribution of other terms results in expression

$$\langle N_{apx}(t) \rangle = \langle N_m(t) \rangle - \langle C_{m+1}(t) \rangle - \langle C_{m-1}(t) \rangle\,, \tag{15}$$

where $\langle N_m(t) \rangle = \langle P(t-t_0) \rangle_{t_0}$ is defined in Eq. (8) of the main part of the paper and

$$\langle C_{m\pm1}(t) \rangle = 2J_{m\pm1}(p) \Big\{ \cos\psi_{m\pm1}(t) - e^{-B} \cos\left[\psi_{m\pm1}(t) \pm D\right] - J_m(p) \left[\cos(\Omega t + \varphi) - e^{-B} \cos(\Omega t + \varphi + D)\right] \Big\}, \tag{16}$$

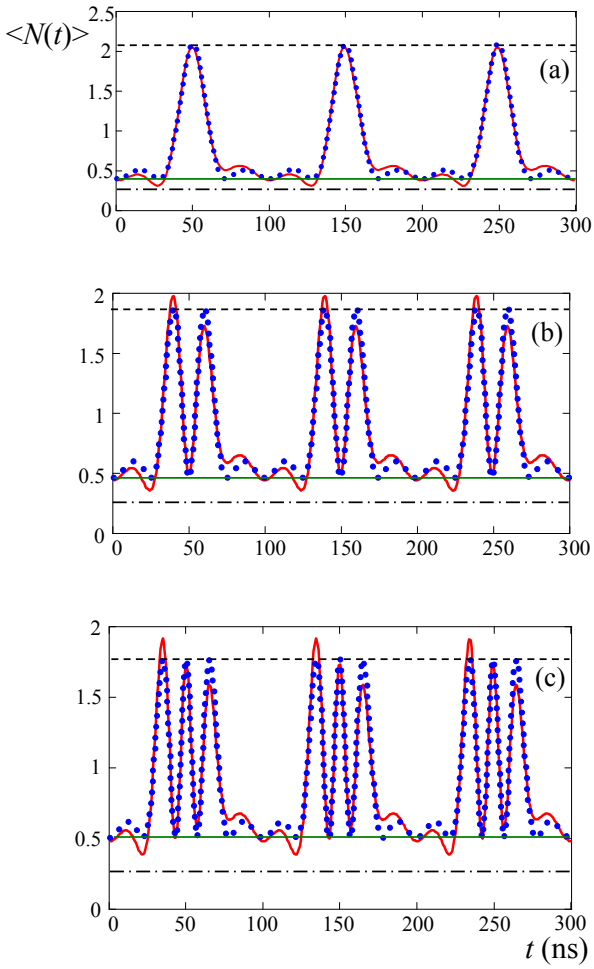

FIG. 3: (color on line) Time dependence of the photon counts, averaged over t_0, for $\Delta = \Omega$ and $p = 1.8$ (a), $\Delta = 2\Omega$ and $p = 3.1$ (b), $\Delta = 3\Omega$ and $p = 4.2$ (c). Solid line (in red) represents the exact result and dotted line (in blue) - analytical approximation, Eq. (8) from the main part of the paper. Dashed black line shows the level $\langle N_m \rangle_{max}$, solid line (in green) - $\langle N_m \rangle_{min}$, and dash-dotted line represents $\langle N \rangle_{res}$. Other parameters are defined in the text.

$$B + iD = \frac{b}{2\gamma - i\Omega}. \tag{17}$$

It is easy to show that the contribution of terms $\langle C_{m\pm1}(t) \rangle$ is as small as $2b\gamma/\Omega^2$ if $\Omega \gg 2\gamma$ and $\Omega \gg b$. However, in spite of the smallness of the corrections, Eq. (15) describes much better the formation of pulses than the analytical approximation Eq. (8) in the main part of the manuscript, see Fig. 4, where Eq. (15) is compared with the exact result. Misfit between them is almost negligible.

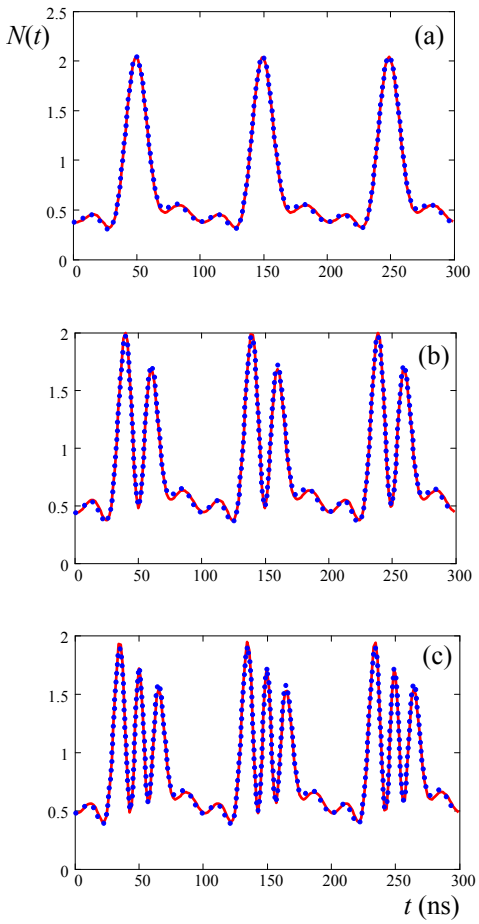

FIG. 4: (color on line) Comparison of the exact result (solid line in red) for time dependence of the photon counts, averaged over t_0, for $\Delta = \Omega$ and $p = 1.8$ (a), $\Delta = 2\Omega$ and $p = 3.1$ (b), $\Delta = 3\Omega$ and $p = 4.2$ (c) with analytical approximation Eq. (15) (dotted line in blue). Other parameters are the same as in Fig.1 (a-c) of the main part of the manuscript.

II. PHASE EVOLUTION AND FORMATION OF PULSES AND DARK WINDOWS

Time dependence of phase $\psi_m(t)$ is shown in Fig. 5 for $m = 1$ (a), $m = 2$ (b), and $m = 3$ (c) if $\varphi = 0$ and modulation index p has optimal value for each m. The phase $\psi_m(t)$ evolves almost linearly as $(m + p)\Omega t + C$ during the pulse (pulses) formation around $\Omega t_p = (2n + 1)\pi$ (C is constant within each time interval), and the phase evolution almost stops around $\Omega t_s = 2n\pi$. Durations of linear time evolution and the phase stopping intervals are nearly equal each other and they are nearly confined within the time intervals ($\Omega t_p -$

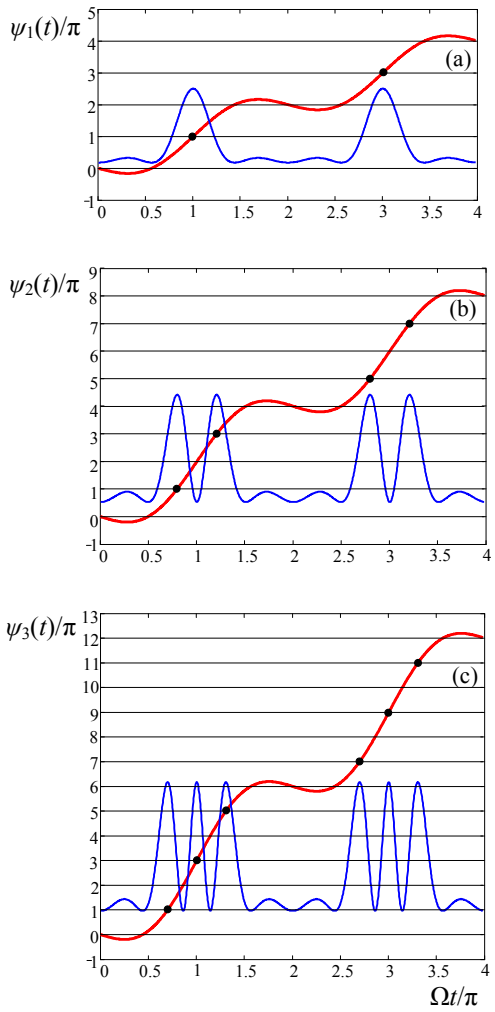

FIG. 5: (color on line) Time evolution of the phase difference of the comb and resonantly scattered field component, $\psi_m(t)$, for $m = 1$ (a), $m = 2$ (b), and $m = 3$ (c), thick line in red. Black circles indicate the points when $\psi_m(t) = (2n + 1)\pi$. The values of the modulation index are taken the same as in Fig. 1. The modulation phase is $\varphi = 0$. Thin solid line in blue shows the formation of pulses according to Eq. (5) in the main part of the manuscript. For visualization the exponential factor is removed and time dependent Bessel function is set equal to zero. The amplitudes of the pulses are scaled to fit a half of each plate.

$\pi/2, \Omega t_p + \pi/2)$ and $(\Omega t_s - \pi/2, \Omega t_s + \pi/2)$, respectively. The phase stops could be explained by "destructive interference" of two terms in expression for the phase $\psi_m(t)$ at the optimal values of the modulation indexes since at the stops the phase evolution is approximated as $(m-p)\Omega t + C$. Actually these "phase stopping" periods are the periods when time evolution

of $\psi_m(t)$ changes the slope from $(m+p)\Omega t$ to $(m-p)\Omega t$. Since for the optimal values of the modulation index p we have $p > m$ and approximately the relation $p \approx m+1$ is valid, then the slope of the phase change during formation of pulses is $(2m+1)\Omega t$ and this slope is negative, $-\Omega t$, during the dark windows.

III. OPERATIONS WITH TIME BIN QUBITS

Here we consider two algorithms how pulse bunching can be used to create and operate with time bin qubits. Assume that the phase of absorber vibrations is zero, $\varphi = 0$, and we tune the radiation source in resonance with the first satellite, $\omega_s = \omega_a + \Omega$. Then the pulses are formed at the moments of time $t_p = (2n+1)T_v/2$, where T_v is the period of the vibrations and $n = 0, 1, 2...$ The dark windows are formed around the moments of time $t_d = nT_v$. The illustration of these pulses and dark windows is given in Fig. 6a. In the bottom panel, Fig. 6d, the evolution of the radiation phase, $\sin(\Omega t)$, is shown. It is divided into bins A and B. The A bins are centered at times t_p where the pulses are formed due to constructive interference of the incident and coherently scattered radiation fields. The B bins are centered at times t_d where dark windows appear due to destructive interference of the incident and coherently scattered radiation fields. The length of these bins is equal to half a period of the vibrations, $T_v/2$. Below we assume that we have a local oscillator, for example, a generator producing the voltage oscillating according to the function $\sin(\Omega t+\varphi_{lo})$ with phase $\varphi_{lo} = 0$. The same oscillator generates mechanical vibrations of the absorber with tunable phase φ. If $\varphi = 0$, all the pulses are formed at the output of the absorber in A bins and dark window are located in B bins (see Fig. 6a). If $\varphi = \pi$ the pulses are generated in B bins, while dark windows are located in A bins (see Fig. 6b). If $\varphi = \pi/2$, then the radiation field is equally distributed among A and B bins (see Fig. 6c).

In optical domain such bins can be spatially separated by router based, for example, on the Mach-Zehnder interferometer with a phase shifter placed in one of the interferometer arms. If this phase shifter is fed by the local oscillator, one can send the radiation field from bins A to the detector A and from bins B to the detector B in accordance with the phase evolution shown in Fig. 6d. If the phase modulator of the radiation field, placed between the source and absorber to create a frequency comb, has the modulation phase φ, which is the same as $\varphi_{lo} = 0$, then only the detector A will detect the radiation field. If this phase

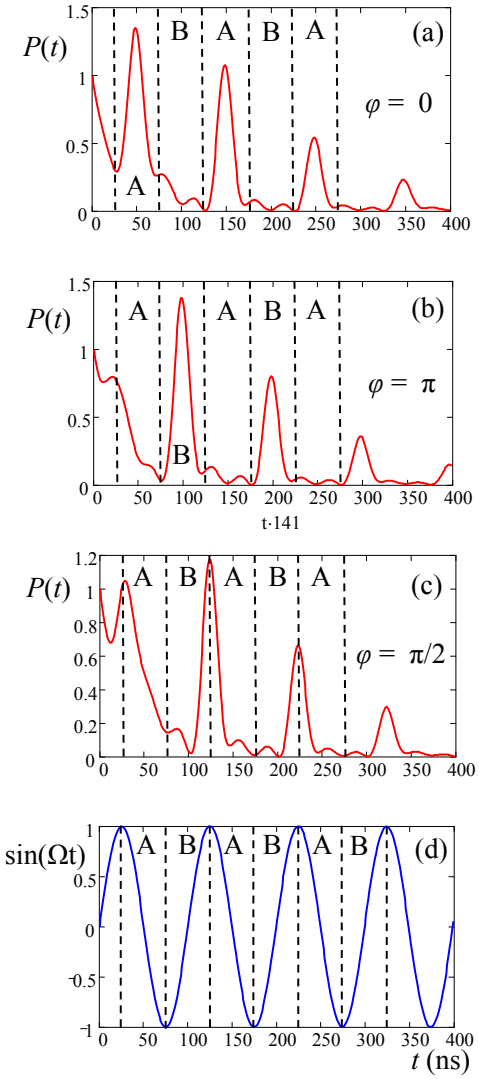

FIG. 6: (color on line) (a)-(c) Time dependence of the detection probability of a photon, which is in resonance with the first satellite of the central component of the frequency comb, $\omega_s = \omega_a + \Omega$. The vibration frequency of the absorber is $\Omega = 10$MHz and the modulation index is $p = 1.8$. Effective thickness of the absorber is $T = 12$. The value of the vibration phase φ is indicated in each plot. (d) The phase evolution of the field interacting with the vibrating absorber in its reference frame. Dashed vertical lines separate time bins A and B (see the text for details).

has a π shift with respect to $\varphi_{lo} = 0$, only the detector B will detect the radiation field. If the modulation phase is $\pi/2$, both detectors have the same probability of photon detection. In such a way we propose to create time bin qubit, which is equivalent to spin 1/2.

In gamma domain the routers are not currently available. However, main elements,

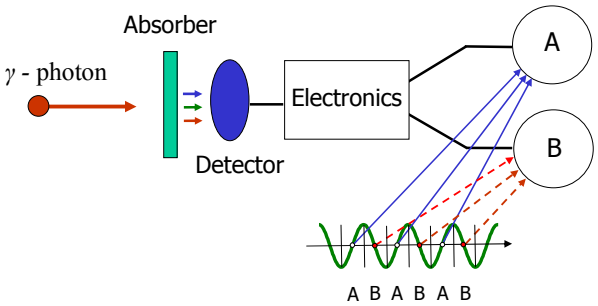

FIG. 7: (color on line) Schematic presentation of the method how with one detector (dark oval in blue) the pulses, formed by the vibrating absorber from single gamma-photon, can be transferred by electronics (data acquisition system) into bins A and B. The correspondence of these bins to the time evolution of the oscillating phase (waving line in green) is shown in the bottom.

from which they could be constructed, are recently developed. They are high-efficient back-reflecting mirrors [7], efficient beam-splitters [8], tight focusing facilities [9], and cavities [10]. Meanwhile, even without routers we can distinguish A and B bins electronically (see Fig. 7). In time delayed coincidence counting technique we have only two detectors. One is for the heralding 122 keV photon, which starts the clock, and the other is for the resonant 14.4 keV photon, which stops the clock. We distinguish detection events of 14.4 keV photon in time by multichannel data acquisition system with quite short duration of each channel (see, for example, Ref. [1, 11]). This scheme can be easily modified to simulate effective detectors A and B electronically, having physically only one detector for the resonant gamma photon.

We assume that in optical domain it is possible to organize qubits of higher dimension, known as qudits, by transformation of a single photon into bunches of pulses and by routers. We estimate that it would be hard to vibrate the absorber piston like with large amplitude comparable with the wavelength of the optical radiation field. The simplest way to organize the phase modulation of the radiation field with high frequency and large deviations is the use of phase modulators. If the modulation index is large enough the single frequency radiation field is transformed into a frequency comb with desirable properties. As an example we consider the case when the second satellite of the central component of the radiation field incident to the absorber is tuned in resonance, $\omega_s = \omega_a + 2\Omega$, and modulation index has optimal value $p = 3.1$, i.e., it is close to π. Then the single-photon wave packet after passing through the absorber is split into bunches of pulses with two pulses in each bunch (see Fig.

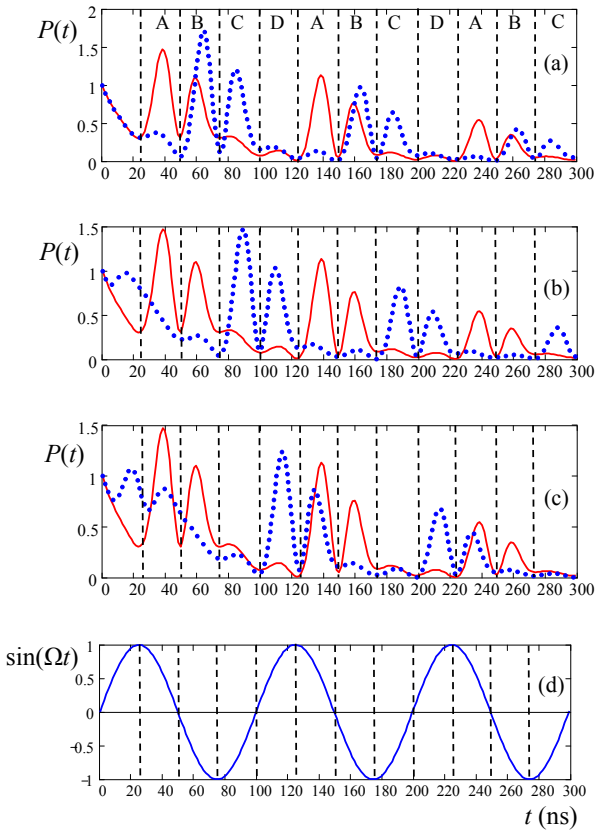

FIG. 8: (color on line) (a)-(c) Time dependence of the detection probability of a photon with comb spectrum, whose second satellite of the central component is in resonance with the absorber, $\omega_s = \omega_a + 2\Omega$. Frequency of the phase modulation is $\Omega = 10$MHz and the modulation index is $p = 3.1$. Effective thickness of the absorber is $T = 12$. The value of the modulation phase φ is zero for solid line (in red) and it is $-\pi/2$ (a), $-\pi$ (b), and $-3\pi/2$ (c) for dotted lines (in blue). (d) The phase evolution of the field after the phase modulator (normalized to the modulation index p) if $\varphi = \varphi_{lo} = 0$. Dashed vertical lines separate time bins A, B, C, and D (see the text for details).

8a, solid curve in red). Now, time can be grained into time bins A, B, C, and D with a duration $T_v/4$ each. If the phase of the phase modulation (PM) is zero, $\varphi = 0$, i.e. it coincides with the phase of the local oscillator, φ_{lo}, then only bins A and B contain the radiation pulses, while bins C and D fall into dark windows (see Fig. 8a, solid curve in red). If the phase of PM is $\varphi = -\pi/2$, the pulse bunches are shifted to a quarter of modulation period and then bins B and C are occupied while bins A and D are almost empty (see Fig. 8a, dotted line in blue). Changing the modulation phase further ($\varphi = -\pi$) we can

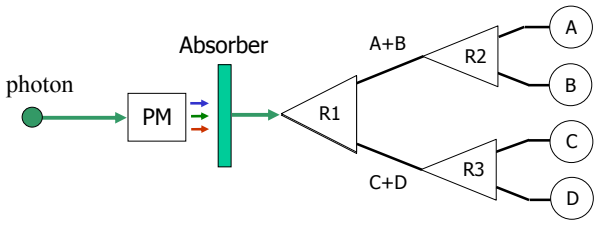

FIG. 9: (color on line) Spatial separation of pulses from bunches. Single photon radiation field is transformed to the frequency comb by phase modulator PM. Passing through the absorber the single photon wave packet is shaped into pulses, which are spatially separated by routers R1, R2, and R3 such that bins A, B, C, and D are sent to the corresponding detectors A, B, C, and D (see the text for details).

move pulses from bins B and C to bins C and D (see Fig. 8b, dotted line in blue). If the modulation phase is $\varphi = -3\pi/2$, the pulses occupy D and A bins only (see Fig. 8c, dotted line in blue).

To separate spatially time bins A, B, C, and D we propose to transmit the radiation field through a set of routers R1, R2, and R3 (see Fig. 9). Router 1 (R1) separates the couple of time bins A and B from couple of time bins C and D. R1 is synchronized with the local oscillator such that the first half a period T_{lo} of the local oscillator the radiation field is sent to the router R2 and the second half of the oscillation period the radiation field is sent to the Router 3. These routers, R2 and R3, switch the path of the radiation field two times faster than R1 but with the same phase φ_{lo}. Then the radiation field, contained in time bin A, will always go to the detector A. The same is realized for time bins B, C, and D. The radiation field contained in these time bins will go to the detectors B, C, and D, respectively (see Fig. 9). By changing the phase of PM, φ, with respect to the phase of local oscillator, φ_{lo}, one can control the population of bins A, B, C, and D.

It is interesting to notice that single pulses, generated when we tune in resonance the first satellite (see Fig. 6), are in phase with the incident radiation field. When we tune in resonance the second satellite, two pulses are grouped in a bunch (see Fig. 8). The first pulse in a bunch has a phase shift $\pi/2$ with respect to the incident field and the second pulse has opposite phase, $-\pi/2$. This feature could be used to implement some operations with bins A, B, C, and D if we make them interfere after passing appropriate bins through

a delay line.

[1] R.N. Shakhmuratov, F. Vagizov, J. Odeurs, and O. Kocharovskaya, Phys. Rev. A **80**, 063805 (2009).

[2] E. Ikonen, P. Helisto, T. Katila, and K. Riski, Phys. Rev. A **32**, 2298 (1985).

[3] F. J. Lynch, R. E. Holland, and M. Hamermesh, Phys. Rev. **120**, 513 (1960).

[4] M. D. Crisp, Phys. Rev. A **1**, 1604 (1970).

[5] E. Varoquaux, G. A. Williams, and O. Avenel, Phys. Rev. B **34**, 7617 (1986).

[6] E. Kuznetsova, R. Kolesov, and O. Kocharovskaya, Phys. Rev. A **68**, 043825 (2003).

[7] Yu. Svid'ko, S. Stoupin, V. Blank, S. Terentyev, Nature Photon. **5**, 539 (2011).

[8] T Osaka, M. Yabashi, Y. Sano, K. Tono, Y. Inubushi, T. Sato, S. Matsuyama, T. Ishikawa, and K. Yamauchi, Opt. Express **21**, 2823 (2013).

[9] F. Döring, A.L. Robisch, C. Eberl, M. Osterhoff, A. Ruhlandt, T. Liese, F. Schlenkrich, S. Hoffmann, M. Bartels, T. Salditt, and H.U. Krebs, Opt. Express **21**, 019311 (2013).

[10] J. Chen, I. V. Tomov, A. O. Er, and P. M. Rentzepis, Appl. Phys. Lett. **102**, 174101 (2013).

[11] R. N. Shakhmuratov, F. Vagizov, and O. Kocharovskaya, Phys. Rev. A **84**, 043820 (2011).

Transformation of a single photon field into bunches of pulses

R.N. Shakhmuratov,[1,2] F.G. Vagizov,[1,2,3] V.A. Antonov,[2,4,5] Y.V. Radeonychev,[4,5] and O. Kocharovskaya[3]

[1]*Kazan Physical-Technical Institute, Russian Academy of Sciences, 10/7 Sibirsky Trakt, Kazan 420029 Russia*
[2]*Kazan Federal University, 18 Kremlyovskaya Street, Kazan 420008 Russia*
[3]*Department of Physics and Institute for Quantum Studies, TAMU, College Station, Texas 77843-4242, USA*
[4]*Institute of Applied Physics of the Russian Academy of Sciences, Nizhny Novgorod 603950, Russia*
[5]*N.I. Lobachevsky State University of Nizhny Novgorod, Nizhny Novgorod, 603950, Russia*

(Dated: December 17, 2014)

We propose a method to transform a single photon field into bunches of pulses with controllable timing and number of pulses in a bunch. This method is based on transmission of a photon through an optically thick single-line absorber vibrated with a frequency appreciably exceeding the width of the absorption line. The spectrum of the quasi-monochromatic incoming photon is 'seen' by the vibrated absorber as a comb of equidistant spectral components separated by the vibration frequency. Tuning the absorber in resonance with m-th spectral component transforms the output radiation into bunches of pulses with m pulses in each bunch. We experimentally demonstrated the proposed technique with single 14.4 keV photons and produced for the first time gamma-photonic time-bin qudits with dimension $d = 2m$.

PACS numbers: 42.50.Gy

arXiv:1412.4611v2 [quant-ph] 16 Dec 2014

Introduction. Rapid development of quantum information technologies demands to invent and bring into routine new methods to control and process single photons. In vast majority of quantum protocols photon polarization is used as the information carrier, see, for example, review [1]. Time-bin qubits, proposed and implemented in Refs. [2, 3], were practically the first examples how time domain can be involved into the information coding by splitting a single photon into two pulses with a fixed phase difference. The information carried by such a photon is well protected during its propagation in optical fiber since cross talk, usually influencing polarization states of a photon, is excluded. Information coding [2, 3] is implemented by the interferometer having different lengths of the arms and a phase shifter placed in the long arm of the interferometer. Unbalanced three path interferometers were used in [4] to create qutrits. Recently, new methods to process time-bin qubits [5, 6] and to create time-bin qubits, qutrits, and ququads [7] were reported.

In this paper we propose to split a photon in time bins by transmission through a thick resonant absorber experiencing phase modulation of its interaction with the field. We test our proposal in gamma domain where a single photon is produced by a naturally decaying nucleus. Radioactive ^{57}Co is ideal for test experiments since coherence length of produced photons is incredibly long and falls into domain where simple electronics may be applied to treat experimental data. The source containing these nuclei is commercially available and relatively cheap. Moreover, the detectors in gamma domain have high quantum efficiency and almost no dark counts. Our method to control the shape of a single-photon wave packet is applicable to all spectral domains, including optical domain where atoms may play a role of optical memory and processors for quantum information. The modulation of the atom-field interaction in optical domain can be realized by Zeeman/Stark effects, as it was discussed in Refs. [8, 9] in connection with a proposal of the new technique to produce extremely short pulses, or by phase modulators. The method is flexible to make fine tuning the amplitudes, time, and intervals between pulses produced from a single photon.

We have to mention the currently available experimental techniques, developed for the single gamma-photon waveform shaping, which could be also applied to extend the methods of quantum information processing. They include magnetic switching [10–13], modulation technique [14, 15], and step-wise phase modulation of the radiation field [16–22].

Basic idea. Single photon, emitted by a source nucleus, has a Lorenzian spectrum whose width is mostly defined by the lifetime of the excited state nucleus. We transmit such a photon through a thick resonant absorber with a single resonance line having approximately the same width as the spectrum of the radiation field. The absorber experiences periodic mechanical vibrations along the photon propagation direction. They are induced by the piezoelectric transducer. In the reference frame of the piston-like vibrating absorber the field phase oscillates as $(2\pi\delta/\lambda)\sin\Omega t$, where Ω and δ are the frequency and amplitude of the periodical displacements, λ is the wavelength of the radiation field. The probability amplitude of the radiation field in the laboratory reference frame, $a_L(t,z) = a_0(t)\exp(-i\omega_s t + ik_s z)$, is transformed to $a_A(t,z) = a(t,z)_L \exp[ip\sin(\Omega t + \varphi)]$ in the vibrating absorber reference frame. Here ω_s, k_s are the frequency and wave number of the radiation field, z is a coordinate on the axis $\mathbf{z}$, along which the photon propagates, $p = 2\pi\delta/\lambda$ is the modulation index, and φ is the relative phase of the absorber vibration. The probability

amplitude $a_A(t,z)$ can be expressed as

$$a_A(t,z) = a_L(t,z) \sum_{m=-\infty}^{+\infty} J_m(p) e^{im(\Omega t+\varphi)}, \qquad (1)$$

where $J_m(p)$ is the Bessel function of the m-th order. From this expression it is obvious that the vibrating absorber 'sees' the incident radiation field as an equidistant frequency comb with spectral components $\omega_s - m\Omega$ having Lonrenzian shape each and intensities, which are proportional to $J_m^2(p)$. Let us say that the m-th component of this field is tuned in resonance with the absorber. If the halfwidth of the components γ_s (it is defined by the halfwidth of the spectrum of the incident field, $a_L(t,z)$) is much smaller than the distance between neighboring components, Ω, then we may assume that only resonant component interacts with the absorber and others pass through without interaction. Within the adopted approximation only the interacting component is coherently scattered by nuclei of the absorber. For week fields the output radiation field can be expressed as a sum of the incident and coherently scattered radiation fields [23]. In case of a single-line resonant radiation these fields interfere destructively, resulting in the radiation damping. For the frequency comb only the resonant component is coherently scattered by resonant nuclei and the scattered field interferes with the whole frequency comb at the exit of the absorber. Therefore the output radiation field reveals unusual properties.

The shape of a single photon wave-packet is described by the exponentially decaying function with the rate γ_s,

$$a_L(t-t_0) = \Theta(t-t_0)\exp[-(i\omega_s+\gamma_s)(t-t_0)+ik_s z], \quad (2)$$

where $\Theta(t-t_0)$ is the Heaviside step function and t_0 is the moment of time when the excited state of the source nucleus is formed. Such a shape is typical for single photon wave-packets if we know the time of formation of the excited state particle producing this single photon (see, for example Refs. [24, 25]). In our case we also know this time to be able to reconstruct the photon shape and its following transformation by the absorber. In our experiments the source nucleus, ^{57}Co, decays by electron capture to ^{57m}Fe, which decays in turn by emission of a 122keV photon, followed by a 14.4 keV photon to the ground state ^{57}Fe. In this cascade decay the detection of 122 keV photon heralds the formation of 14.4 keV excited state of ^{57}Fe nucleus in the source (see, for example, Ref. [24]). The absorber contains ground state ^{57}Fe nuclei, which are resonant for 14.4 keV photons.

The propagation of the field, Eq. (2), through a single-line resonant absorber (not vibrating) can be described classically, Ref. [24], or quantum mechanically, Ref. [26]. The result is well known in gamma domain [24, 26] and in quantum optics [27]. In the simplest case if $\omega_s = \omega_a$ and $\gamma_s = \gamma_a$, where ω_a and γ_a are the resonant frequency and halfwidth of the absorption line of the absorber, respectively, the output probability amplitude is

$$a_{out}(t,l) = a_L(t,l) J_0\left(2\sqrt{bt}\right), \qquad (3)$$

where l is the physical thickness of the absorber, $t_0 = 0$, and t is the local time $t - l/c$. Below we disregard this retardation since physical length of the absorber is small and retardation time l/c is short with respect to the time scale of the amplitude evolution. The parameter $b = \gamma_a T_a/2$ is defined by the product of the decay rate of the nuclear coherence γ_a and optical depth of the absorber, which is $T_a = \alpha_B l$, where $\alpha_B = N\sigma$ is the Beer's law absorption coefficient applicable to a monochromatic radiation tuned in resonance, N is the density of ^{57}Fe nuclei in the absorber, and σ is the cross section of resonant absorption for 14.4 keV transition. The inverse value of b is usually referred to as superradiant time, $T_{SR} = 1/b$. Here we disregard recoil processes in nuclear absorption and emission assuming that recoilless fraction (Deby-Waller factor) is $f_a = 1$. These processes will be taken into account for experimental data treatment.

Since we are interested only in the detection probability of a photon, which is equivalent to the radiation intensity, the cases when the absorber vibrates with respect to the source at rest or vice versa give the same result. For simplicity we consider the case of the vibrating source. Then, the radiation field at the exit of the absorber at rest is the sum of the comb, Eq. (1), and the coherently scattered field. We suppose that the frequency component $\omega_s - m\Omega$ is in resonance with the absorber. Then, according to Eq. (3) the probability amplitude of the coherently scattered field is

$$a_{sct}(t,l) = a_L(t,l) S_m(t) e^{im(\Omega t+\varphi)}, \qquad (4)$$

where $S_m(t) = J_m(p)\left[J_0\left(2\sqrt{bt}\right) - 1\right]$. This field is just the output field $a_{out}(t,l)$ for the component $a_L(t,z)J_m(p)\exp[im(\Omega t+\varphi)]$ minus this component if it would propagate without interaction with the absorber [21, 28]. Simple calculation of the probability $P(t) = |a_L(t,l) + a_{sct}(t,l)|^2$ of the output radiation field gives

$$P(t) = \Theta(t) e^{-2\gamma t}\left[1 + 2S_m(t)\cos\psi_m(t) + S_m^2(t)\right], \quad (5)$$

where $\gamma = \gamma_a = \gamma_s$ and $\psi_m(t) = m(\Omega t+\varphi) - p\sin(\Omega t+\varphi)$. Time evolution of the probability $P(t)$ for $m = 1$, 2, and 3, is shown in Fig. 1 (a, b, and c, respectively) where the results of approximate Eq. (5) are compared with the exact expression $P_{ext}(t) = |a_{ext}|^2$, which is obtained if we calculate the probability amplitude without any assumptions (see, for example, Ref. [19]), i.e.,

$$a_{ext}(t,l) = a_A(t,l) - b\int_0^t a_A(t-\tau,l) j_1(b\tau) e^{-\gamma_a\tau - i\omega_a\tau} d\tau, \qquad (6)$$

where $j_1(b\tau) = J_1\left(2\sqrt{b\tau}\right)/\sqrt{b\tau}$. Small misfits can be almost excluded if we take into account the contribution of the two neighboring satellites, both red and blue detuned from the resonant component of the comb, see Supplemental Material (SM).

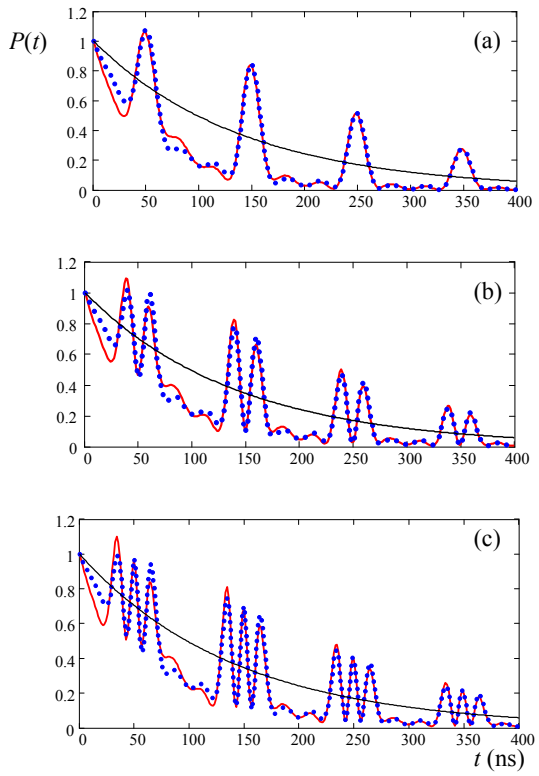

FIG. 1: (color on line) Time dependence of the detection probability of a photon, $P(t)$, at the exit of the absorber vibrating with the frequency $\Omega = 10$ MHz and phase $\varphi = 0$. Optical thickness of the absorber is $T = 5.2$ and $\gamma_a = \gamma_s = 1.13$ MHz. The frequency of the radiation field ω_s is tuned in resonance with the first sideband $\omega_a+\Omega$ (a), the second sideband $\omega_a+2\Omega$ (b), and the third sideband $\omega_a+3\Omega$ (c). The value of the modulation index is taken optimal in each case, i.e., $p_1 = 1.8$ (a), $p_2 = 3.1$ (b), and $p_3 = 4.2$ (c), (see the text). Dotted line (in blue) corresponds to the analytical approximation (5) and solid line (in red) demonstrates the result obtained from the exact solution (6).

We see that the shape of the photon wave packet is transformed into bunches of pulses with the number of pulses per bunch equal to m. The pulses are produced due to constructive interference of the incident field with coherently scattered field when $\psi_m(t) = (2n+1)\pi$, $n = 0, 1, 2, ...$, while the dark windows appear due to destructive interference when $\psi_m(t) = 2n\pi$, if $S_m(t)$ is negative in both cases. The probability has maxima, corresponding to pulses, $[1-S_m(t)]^2 \exp(-2\gamma t)$ and minima $[1+S_m(t)]^2 \exp(-2\gamma t)$, relevant to the radiation drop. The most pronounced pulses appear if the intensity of the resonant component $[\sim J_m^2(p)]$ has global extremum. For example, the maxima, predicted by Eq. (5) without exponential factor $\exp(-2\gamma t)$ and assuming that $J_0\left(2\sqrt{bt}\right) \approx 0$, which means that the scattered field had time to fully develop, are $[1+J_1(p_1)]^2 = 2.5$ if $p_1 = 1.8$; $[1+J_2(p_2)]^2 = 2.1$ if $p_2 = 3.1$; and $[1+J_3(p_3)]^2 = 2.06$ if $p_3 = 4.2$, i.e., the intensity of the pulses exceeds almost two times the intensity of the radiation field if it would not interact with the absorber. The radiation field between bunches is quite small because of destructive interference, for example, $[1-J_1(p_1)]^2 = 0.175$ if $p_1 = 1.8$; $[1-J_2(p_2)]^2 = 0.26$ if $p_2 = 3.1$; and $[1-J_3(p_3)]^2 = 0.32$ if $p_3 = 4.2$, i.e., almost an order of magnitude smaller with respect to the pulse maxima. Qualitatively the appearance of bunches can be understood from the time evolution analysis of the phase difference of the scattered field and the comb, which is $\psi_m(t)+\pi$ if $S_m(t) < 0$. The phase $\psi_m(t)$ evolves almost linearly as $(m+p)\Omega t+C$ during the pulse (pulses) formation around $\Omega t_p = (2n+1)\pi$ (C is constant within each time interval), and the phase evolution almost stops around $\Omega t_s = 2n\pi$, see SM for details.

It is interesting to notice that tuning in resonance the $m = -1$ component (if $\varphi = 0$) shifts the position of the pulses with respect to the case of $m = +1$ such that maxima become minima and vice versa. Such a difference is explained by the fact that the amplitude of the $m = -1$ component of the comb is proportional to $J_{-1}(p) = -J_1(p)$ and hence the amplitude of the antiphase scattered field [proportional to $S_{-1}(t)$] becomes positive. The details how to move the radiation field from one time-bin to the other time-bin by changing the phase φ and how this effect can be used to create time-bin qubits and qudits are discussed in SM.

Experiment. The details of the experimental setup are described in Refs. [21, 28]. Recently we developed a new scheme of photon counts selection and reported our first observation of photon shaping into a series of short single-pulse bunches [15]. This transformation is performed by tuning the radiation source in resonance with the first sideband $m = 1$. Below we sketch out the experimental scheme.

The radiation source is a radioactive ^{57}Co in rhodium matrix. The absorber is a 25-μm-thick stainless-steel foil with a natural abundance ($\sim 2\%$) of ^{57}Fe. Optical depth of the absorber is $T_a = 5.18$. The stainless-steel foil is glued on the polyvinylidene fluoride piezotransducer that transforms the sinusoidal signal from radio-frequency generator into the uniform vibration of the foil. The tuning of the source in resonance for the preselected component of the spectrum is performed by Mössbauer transducer working/running in constant velocity mode. The source is attached to the holder of the Mössbauer transducer causing Doppler shift of the radiation field. Two detectors, D1 and D2, are used in data acquisition scheme. D1 (shielded by copper foil) detects only heralding 122 keV photons in a cascade decay, 122 keV and 14.4 keV, of ^{57}Co. This detector starts the clock. Detection of 14.4 keV photon by D2 stops the clock. In this time-delayed coincidence count technique we reconstruct the time evolution of the photon wave packet transmitted through the resonant absorber. Since time t_0 of the formation of 14.4 keV state nucleus in the source is random, we select only those counts of the heralding 122 keV photons, which are detected within

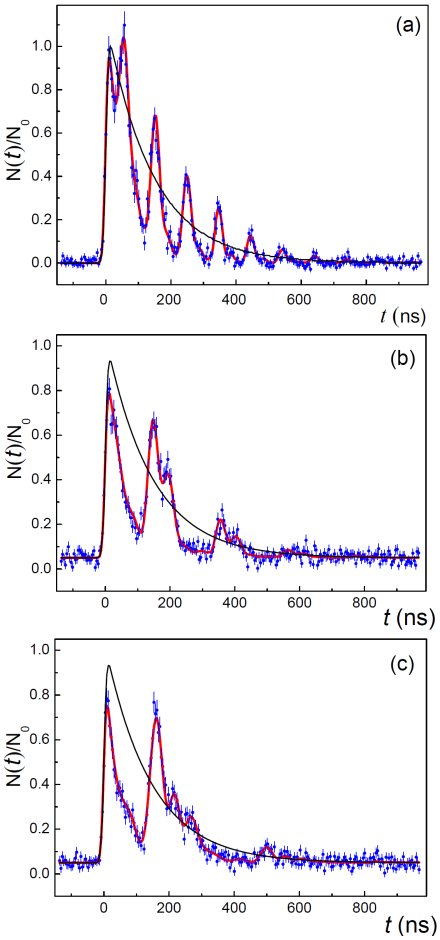

FIG. 2: (color on line) Time dependence of the photon counts $N(t)$ at the exit of the absorber vibrating with the frequency $\Omega = 10.2$ MHz (a), $\Omega = 4.79$ MHz (b), and $\Omega = 2.94$ MHz (c). $N(t)$ is normalized to the value N_0 without resonant absorbtion if the contribution of nonresonant photons with recoil is subtracted. The frequency of the radiation field ω_s is tuned in resonance with the first sideband $\omega_a + \Omega$ (a), the second sideband $\omega_a + 2\Omega$ (b), and the third sideband $\omega_a + 3\Omega$ (c). Solid line (in red) corresponds to the theoretical fitting, which takes into account the phase jitter. The modulation index, the phase, and the phase jitter $\Delta\varphi$ are $p = 1.8$, $\varphi = 0$, and $\Delta\varphi = \pi/2$ (a), $p = 3.08$, $\varphi = 0$, and $\Delta\varphi = \pi/3$ (b), $p = 4.21$, $\varphi = -\pi/10$, and $\Delta\varphi = \pi/5$ (c). The dots with error bars (in blue) show experimental points. Thin line (in black) shows the probability time dependence without absorber.

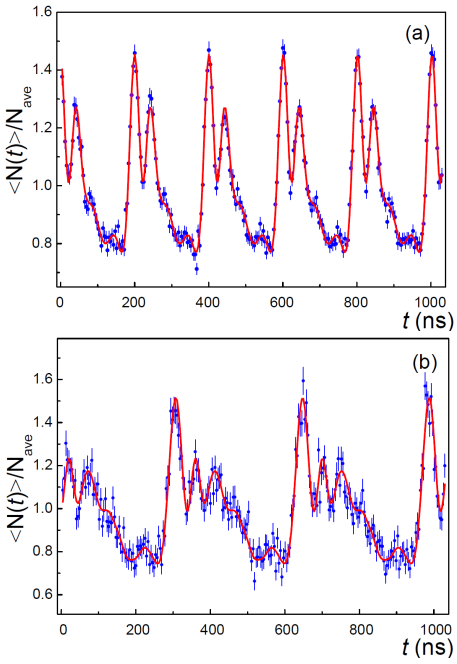

FIG. 3: Time dependence of the t_0 averaged detection probability of a photon, $\langle N(t)\rangle \sim \langle P(t)\rangle_{t_0}$, at the exit of the vibrating absorber. N_{ave} is the averaged count rate. The experimental conditions and notations in plots (a) and (b) are the same as in plots (b) and (c) in Fig. 2, respectively. The experimental results are fitted to the exact calculation of the integral in Eq. (7), see the details in SM.

short time interval Δt around time t_{ph} satisfying the relation $\Omega t_{ph} = \varphi + 2\pi n$, where n is integer. This selection secures that the phase of the absorber vibration is always the same for all detected photons. Since small time window of count selection Δt is not zero, we have to average the theoretical expressions for the signal $P(t)$ over small jitter $\Delta\varphi$ of phase φ caused by finite value of Δt.

Time resolution of the electronics in our setup is 8 ns and hence time structures shorter than 8 ns would be not resolved. In Ref. [15] we modulated the absorber with frequency $\Omega = 10.2$ MHz and tuned the radiation field in resonance with the first satellite. We observed pulses as short as 30 ns, which are artificially broadened due to $\Delta\varphi \neq 0$. If we tune the source in resonance with the second or third satellite and keep the same frequency of modulation $\Omega = 10.2$ MHz, the pulses will be 2 or 3 times shorter, respectively (see Fig. 1), which makes difficult to resolve pulses within the bunches. To be able to resolve the content of the pulse bunches, for example, consisting of two or three pulses, we had to reduce Ω two or three times, respectively, compared to the modulation frequency, used in our first experiment. The experimental results of the detecting of pulse bunching are presented in Fig. 2, where time dependence of the number of counts $N(t)$, normalized to the maximum value N_0 without absorber, is shown. The ratio $N(t)/N_0$ is proportional to the probability $P(t)$. The details of fitting procedure are described in Ref. [15].

To avoid smearing out of the pulses within the bunch we performed experiments where time t_0 is still random but we count time delay of 14.4 keV photon detection by the detector D2 with respect to the fixed moments of time when the modulation phase φ is the same (differing only in $2\pi n$). Thus, we don't use detector D1 and time delay of the detection of 14.4 keV photon, t_{stop}, is counted with respect to a fixed t_{start}, which is not random. In this way we escape an artificial phase jitter $\Delta\varphi$ inherent

to the first scheme of the experiment. What we measure in the modified scheme of experiment is the probability $P(t)$, integrated over time t_0, which varies from $-\infty$ to t, i.e.,

$$\langle P(t-t_0)\rangle_{t_0} = 2\gamma_s \int_{-\infty}^{t} P(t-t_0)dt_0. \qquad (7)$$

Calculation of this integral for the analytical approximation, Eq. (5), gives

$$\langle P(t)\rangle_{t_0} = 1 - 2V_m(p)\cos\psi_m(t) + U_m(p), \qquad (8)$$

where $V_m(p) = J_m(p)[1-\exp(-T_a/4)]$, $U_m(p) = V_m^2(p) + J_m^2(p)\exp(-T_a/2)[I_0(T_a/2)-1]$, and $I_0(T_a/2)$ is the modified Bessel function of zero order. We notice that for a single line absorber (not vibrating) a steady state transmission of resonant gamma-quanta is proportional to the function $\exp(-T_a/2)I_0(T_a/2)$, where T_a is the optical depth of the absorber. Therefore, we conclude that part of the term $U_m(p)$, which is proportional to this function, describes in Eq. (8) a steady state transmission of the resonant m-component of the frequency comb, within the assumption that other components pass through without any change. The exact expression for $\langle P(t-t_0)\rangle_{t_0}$, obtained without analytical approximation (5), looks very complicated and does not allow simple interpretation and analytical analysis, see Ref. [19]. Meanwhile, our approximation slightly deviates from this exact result. However, if the contribution of two neighboring sidebands, blue and red detuned from resonant component, are taken into account, then this difference becomes negligible (see SM).

Figure 3 demonstrates the results of our time-delayed measurements with respect to a fixed phase of the vibrations. In spite of poor time resolution of our electronics the pulses within bunches are clearly seen.

Concluding, we demonstrate a method how to shape single-photon wave packets into bunches of pulses by transmission through the vibrated single-line absorber. We control the number of pulses in a bunch and their timing by tuning the absorber to the proper radiation sideband induced by the absorber vibration.

This work was partially funded by the Russian Foundation for Basic Research (Grant No. 12-02-00263-a), the Program of Competitive Growth of Kazan Federal University funded by the Russian Government, the RAS Presidium Program Quantum Mesoscopic and Disordered Systems, the National Science Foundation (Grant No. PHY-1307346), and the Robert A. Welch Foundation (Award A-1261). We are grateful to Alexey Kalachev for the fruitful discussions.

[1] N. Gisin, G. Ribordy, W. Tittel, and H. Zbinden, Rev. Mod. Phys. **74**, 145 (2002).
[2] J. Brendel, N. Gisin, W. Tittel, and H. Zbinden, Phys. Rev. Lett. **82**, 2594 (1999).
[3] I. Marcikic, H. de Riedmatten, W. Tittel, V. Scarani, H. Zbinden, and N. Gisin, Phys. Rev. A **66**, 062308 (2002).
[4] R.T. Thew, A. Acin, H. Zbinden, and N. Gisin, Phys. Rev. Lett. **93**, 010503 (2004).
[5] P. C. Humphreys, B. J. Metcalf, J. B. Spring, M. Moore, X.-M. Jin, M. Barbieri, W. S. Kolthammer, and I. A. Walmsley, Phys. Rev. Lett. **111**, 150501 (2013)
[6] J. M. Donohue, M. Agnew, J. Lavoie, and K.J. Resch, Phys. Rev. Lett. **111**, 153602 (2013)
[7] B.R. Nisbet-Jones, J. Dilley, A. Holleczek, O. Barter, A. Kuhn, New Journal of Physics **15**, 053007 (2013).
[8] Y.V. Radeonychev, V.A. Polovinkin, O. Kocharovskaya, Phys. Rev. Lett. **105**, 183902 (2010).
[9] V. A. Antonov, Y. V. Radeonychev, O. Kocharovskaya, Phys. Rev, A **88**, 053849 (2013)
[10] Yu.V. Shvydko, S.L. Popov, G.V. Smirnov, Sov. Phys. JETP Lett. **53**, 217 (1991).
[11] Yu. V. Shvyd'ko, T. Hertrich, U. van Bürck, E. Gerdau, O. Leupold, J. Metge, H. D. Rüter, S. Schwendy, G. V. Smirnov, W. Potzel, and P. Schindelmann, Phys. Rev. Lett. **77**, 3232 (1996).
[12] A. Palffy, C. H. Keitel, and J. Evers, Phys. Rev. Lett. **103**, 197403 (2012).
[13] W.T. Liao, A. Pálffy, and C. H. Keitel, Phys. Rev. Lett. **109**, 017401 (2009).
[14] G. V. Smirnov, U. van Bürck, J. Arthur, S. L. Popov, A. Q. R. Baron, A. I. Chumakov, S. L. Ruby, W. Potzel, and G. S. Brown, Phys. Rev. Lett. **77**, 183 (1996).
[15] F. Vagizov, V. Antonov, Y.V. Radeonychev, R.N. Shakhmuratov, and O. Kocharovskaya, Nature **508**, 80 (2014).
[16] P. Helisto, I. Tittonen, M. Lippmaa, and T. Katila, Phys. Rev. Lett. **66**, 2037 (1991).
[17] I. Tittonen, M. Lippmaa, P. Helisto, and T. Katila, Phys. Rev. B **47**, 7840 (1993).
[18] P. Helisto, E. Ikonen, T. Katila, W. Potzel, and K. Riski, Phys. Rev. B **30**, 2345 (1984).
[19] E. Ikonen, P. Helisto, T. Katila, and K. Riski, Phys. Rev. A **32**, 2298 (1985).
[20] P. Schindelmann, U. van Burck, W. Potzel, G. V. Smirnov, S. L. Popov, E. Gerdau, Yu. V. Shvydko, J. Jeschke, H. D. Ruter, A. I. Chumakov, and R. Ruffer, Phys. Rev. A 65, 023804 (2002).
[21] R. N. Shakhmuratov, F. Vagizov, and O. Kocharovskaya, Phys. Rev. A **84**, 043820 (2011).
[22] R. N. Shakhmuratov, F. Vagizov, and O. Kocharovskaya, Phys. Rev. A **87**, 013807 (2013).
[23] R. N. Shakhmuratov, Phys. Rev. A **85**, 023827 (2012).
[24] F. J. Lynch, R. E. Holland, and M. Hamermesh, Phys. Rev. **120**, 513 (1960).
[25] B. Lounis, W.E. Moerner, Nature (London) **407**, 491 (2000).
[26] S. M. Harris, Phys. Rev. **124**, 1178 (1961).
[27] M. D. Crisp, Phys. Rev. A **1**, 1604 (1970).
[28] R.N. Shakhmuratov, F. Vagizov, J. Odeurs, and O. Kocharovskaya, Phys. Rev. A **80**, 063805 (2009).